International Journal of Current Research and Academic Review

ISSN: 2347-3215 Volume 3 Number 8 (August-2015) pp. 208-228

www.ijcrar.com

FT-IR and FT-Raman spectra, HOMO, LUMO, first-order hyperpolarizability and NMR analysis of salicylosalicylic acid based on density functional calculations

V. Krishna Kumar[1], S.Suganya[2]*, R.Mathammal[3] and M.Kumar[4]

[1]Department of Physics, Periyar University, Salem-636 011, India
[2]Department of Physics, N.K.R. Govt. Arts College (W), Namakkal-637 001, India
[3]Department of Physics, Sri Sarada College for Women (Autonomous) Salem-636 016, India
[4]Department of Physics, Govt. Arts College (Autonomous), Salem-636 007, India

Corresponding author

KEYWORDS

Salicylosalicylic Acid, HOMO, LUMO, ^{13}CNMR and ^{1}HNMR, Hyperpolarizability

A B S T R A C T

In the present work, the infrared (IR) and Raman spectra of Salicylosalicylic Acid (abbreviated as SCSA) have been measured in the ranges of 400–4000cm^{-1} and 50–4000cm^{-1}. Optimized geometrical structures, vibrational frequencies, intensities, Mullikan atomic charges and other thermodynamical parameters have been computed by the B3 based (B3LYP) density functional methods using 6-31G*(d,p) basis sets. Reliable vibrational assignments were made on the basis of total energy distribution (TED) calculated with scaled quantum mechanical (SQM) method. The scaled frequencies resulted in excellent agreement with the observed spectral patterns. Lower value in the HOMO and LUMO energy gap explains the eventual charge transfer interactions taking place within the molecule.^{13}C and ^{1}H NMR chemical shifts results were also calculated and compared with the experimental values. The values of electric dipole moment (μ) and the first-order Hyperpolarizability (β) were computed using DFT calculations.

Introduction

Computational studies seem to constitute a valuable tool in pharmaceutical solid-state research. The theory has to be supported by different spectroscopic and diffraction methods. Among them, vibrational spectroscopy is one of the most commonly used for the molecular structure determination.

Quantum chemical computational methods have proven to be an essential tool for interpreting and predicting the vibrational spectra (Hess *et al.*, 1986; Pulay *et al.*, 1993; Hehre *et al.*, 1986; Shin *et al.*, 1998). A significant advancement in this area was made by combining semi-empirical quantum mechanical method; ab initio quantum

mechanical method and density functional theory (DFT), each method having its own advantages (Hehre *et al.,* 1986; Shin *et al.,* 1998; Ziegler, 1991; Blom and Altona, 1976). The aim of this work is to study vibrational (FT-IR, FT-Raman and NMR) spectra and investigated the optimized geometry, atomic charges and vibrational spectra for the title molecules.

Salicylosalicylic acid contains both a hydroxyl and a carboxyl group. Salicylosalicylic acid has also been shown to activate adenosine monophosphate-activated protein kinase (AMPK), and it is thought that this action may play a role in the anticancer effects of the compound and its prodrugs aspirin and salsalate. In addition, the antidiabetic effects of Salicylosalicylic acid are likely mediated by AMPK activation primarily through allosteric conformational change that increases levels of phosphorylation (Hawley *et al.,* 2012). As a consequence, Salicylosalicylic acid may alter AMPK activity and subsequently exert its anti-diabetic properties through altered energy status of the cell. Salicylosalicylic acid has strong antiseptic and germicidal properties because it is a carboxylated phenol. The presence of the carboxyl group appears to enhance the antiseptic property. Many hair tonics and remedies for athlete's foot, corns and warts employ the keratolytic action of Salicylosalicylic acid.

The present work deals with DFT (B3LYP) methods with 6-31G* (d) and 6-31G* (d, p) basis sets using the Gaussian 03W program. We report IR, Raman and ^{1}H, ^{13}C NMR spectroscopic data, HOMO, LUMO and hyperpolarizability of Salicylosalicylic Acid by using DFT/6-31G*(d, p) method. Therefore, we have carried out detailed theoretical and experimental investigation on the vibrational spectra of this molecule completely.

Experimental

The compound under investigation namely Salicylosalicylic acid is purchased from the Lancaster Chemical Company (UK), which is of spectroscopic grade and hence used for recording the spectra as such without any further purification. Fourier transform infrared spectra of the title compound is measured at the room temperature in the 4000-400cm^{-1} region using BRUKER IFS 66V FTIR spectrometer at a resolution of ±1 cm^{-1} equipped with a cooled MCT detector, a KBr beam splitter. The FT-Raman spectrum of SCSA has been recorded using 1064nm line of Nd:YAG laser as excitation wavelength in the region 50–4000cm^{-1} on a BRUKER IFS66v spectrophotometer using KBr pellet technique. The reported wavenumbers are believed to accurate within± cm^{-1}.^{1}H and ^{13}C nuclear magnetic resonance (NMR) (400 MHz; $CDCl_3$) spectra were recorded on a Bruker HC400 instrument. All NMR spectra are measured at room temperature.

Computational details

The most optimized structural parameters, energy, and vibrational frequencies of the molecule have been calculated by using B3 (Becke, 1988) exchange functional combined with the LYP (Lee *et al.,* 1988) correlation functional resulting in the B3LYP density functional method at 6-31G (d, p) basis set. The optimum geometry is determined by minimizing the energy with respect to all geometry parameters without imposing molecular symmetry constraints. The Cartesian representation of the theoretical force constants has been computed at the optimized geometry by the assumption that the molecule belong to C_1 point group symmetry. All the computations were performed using Gaussian 03W program (Frisch *et al.,* 2004) and Gauss-

View molecular visualization program package on the personal computer (Frisch *et al.,* 2007). Multiple scaling of the force field has been performed by the SQM procedure (Rauht and Pulay, 1995; Pulay *et al.,* 1983) to offset the systematic errors caused by basis set incompleteness, neglect of electron correlation and vibrational anharmonicity, the characterization of the normal modes using potential energy distribution (PED) was done with the MOLVIB – 7.0 programs (Sundius, 1990; Sundius, 2002).

The ^{13}C and ^{1}H nuclear magnetic resonance (NMR) chemical shifts of the molecule were calculated by the gauge independent atomic orbital (GIAO) method (Wolinski *et al.,* 1990) at B3LYP method with 6-31G* basis set. The experimental values for ^{1}H and ^{13}C isotropic chemical shifts for TMS were 13.84 and 188.1ppm, respectively (Cheeseman *et al.,* 1996). Furthermore, in order to show nonlinear optic (NLO) activity of title molecule, the dipole moment, linear polarizability and first hyperpolarizability were obtained

The Raman activity (Si) calculated by Gaussian 03 and adjusted during scaling procedure with MOLVIB were converted to relative Raman intensity (Ii) using the following relation from the basic theory of Raman scattering (Polavarapu, 1990; Keresztury *et al.,* 1993).

$$I_i = \frac{f(\upsilon_o - \upsilon_i)^4 S_i}{\upsilon_i \left[1 - \exp\left(\frac{-hc\upsilon_i}{kT}\right)\right]}$$

Where υ_o is the exciting wave number (in cm^{-1} units), υ_i the vibrational wave number of the i^{th} normal mode, h, c, and k are the universal constants and f is a suitably chosen common normalization factor for all peak intensities. For the plots of simulated IR and Raman spectra, pure Lorentzian band shapes were used with a bandwidth (FWHM) of 10 cm^{-1}.

Results and Discussion

Structural properties

In order to find the molecular structure along with numbering of atom of Salicylosalicylic acid (SCSA) is obtained from Gaussian 2003 and Gauss view programs which are shown in figure 1. The optimized geometrical parameters of SCSA obtained using the DFT level of theory are presented in table 1 and the corresponding minimum energy was calculated to be *E* =−915.68208Hartees.The calculated parameters are slightly higher or lower than the experimental values due to the absence of extended hydrogen bonding or the intermolecular stacking interaction in the absolute vacuum. The title compound SCSA belongs to C_1 point group symmetry with 29 atoms. With the electron withdrawing substituents on the benzene ring, the symmetry of the ring is distorted, yielding ring angles smaller than 120^o at the point of substitution and slightly larger than 120^o at the other positions (Wang *et al.,* 1993). The C17–C26 bond length of SCSA is also longer, where the –COOH group is attached. This is due to the electron withdrawing nature of carboxylic acid group.

Vibrational assignments

The maximum number of potentially active observable fundamentals of a non-linear molecule, which contains N atoms, is equal to (3N-6) apart from three translational and three rotational degrees of freedom (Silverstein *et al.,* 1981; Wilson *et al.,* 1980). Hence, SCSA molecule has 29 atoms with 81 normal modes of vibrations and considered under C_1 point group symmetry.

The Eighty-one normal modes of vibrations of SCSA molecule are distributed by symmetry species as:

ΓVib = 55 A (in-plane) + 26 A (out-of-plane)

All the vibrations are active in both Raman scattering and infrared absorption. In the Raman spectrum, the in-plane vibrations give rise to polarized bands while the out-of-plane ones to depolarized band. The observed and calculated infrared and Raman spectra of SCSA are produced in common frequency scales in figures 2 and 3, respectively. The output of the quantum chemical calculations contains the force constant matrix in Cartesian coordinates in Hartree/Bohr^2 units. These force constants are transformed to the force fields in the internal local-symmetry coordinates. The internal coordinates and local symmetry coordinates are given in tables 2 and 3. The assignments of the normal modes of vibrations of the investigated molecules along with the observed fundamentals, unscaled frequencies obtained by B3LYP/6-31G* calculations and scaled frequencies as well as the TED descriptions are reported in table 4 for SCSA.

C–H vibrations

Aromatic compounds commonly exhibit multiple weak bands in the region 3000–3100cm^{-1} (George, 2001) and are of strong to medium intensity and in this study also absorptions in this region are attributed to C–H stretching vibrations. In our present work, the calculated frequencies 3115- 3049 cm^{-1} assigned to the eight C–H stretching vibrations and their experimental counterpart appear in 3087, 3072, 3026,2893,2870 cm^{-1} of the IR spectrum and 3088,3072,3054 cm^{-1} are observed in FT-Raman spectrum for C–H vibrations.

O–H vibrations

The O–H stretching vibrations are sensitive to hydrogen bonding. The O–H stretching vibration is normally observed at about 3300 cm^{-1}. The O–H in-plane bending vibration is observed in the region 1440–1260 cm^{-1} (Sathyanarayan, 2004; Socrates, 2001). In SCSA, the bands appeared at 1247, 1200 cm^{-1} in IR are assigned to O–H stretching modes of vibration.

C =O Vibrations

The C= O stretching bands of acids are considerably more intense than ketonic = O stretching bands, only the asymmetrical C =O stretching mode absorbs in the infrared. Internal hydrogen bonding reduces the frequency of the carbonyl stretching absorption to a greater degree than does intermolecular hydrogen bonding. The carbonyl stretching frequency has been most extensively studied by infrared spectroscopy. This multiple bonded group is highly polar and therefore gives rise to an intense infrared absorption band. The carbon–oxygen double bond is formed by Pπ–Pπ bonding between carbon and oxygen. Because of the different electro negativities of carbon and oxygen atoms, the bonding electrons are not equally distributed between the two atoms. The lone pair of electrons on oxygen also determines the nature of the carbonyl group (Socrates, 2001). In the present study, the very strong band observed at 1739 cm^{-1} in IR for SCSA was assigned to C= O stretching vibrations.

C–O vibrations

If a compound contains a carbonyl group, the absorption caused by the C–O stretching is generally strongest (Bowman *et al.*, 1980). Considerations of these factors lead to assign the band observed at 1561-1220

cm^{-1} to C–O stretching vibrations for the title compound.

Ring vibrations

The ring stretching vibrations are very prominent, as the double bond is in conjugation with the ring, in the vibrational spectra of benzene and its derivatives (Varsanyi, 1969). The carbon–carbon stretching modes of the phenyl group are expected in the range from 1733 to 1250 cm−1. The actual position of these modes is determined not so much by the nature of the substituents but by the form of substitution around the ring (Bellamy, 1975). In general, the bands are of variable intensity and are observed at 1625–1590, 1590–1575, 1540–1470, 1465–1430 and1380–1280 cm−1 from the wavenumber ranges (Varsanyi, 1974) for the five bands in the region. In SCSA, the wavenumbers observed in the FTIR spectrum at 1609,1460-1301 cm^{-1} and in FT-Raman spectrum at 1249,1322,1612,1742 cm^{-1} have been assigned to C–C stretching vibrations. The bands identified at 756,728,668, 645,579, 572, 413, 398, 139, 128, 60 and 59 cm^{-1} for SCSA have been assigned to ring in-plane and out-of-plane bending modes, respectively, by careful consideration of their quantitative descriptions.

Other molecular properties

Charge analysis

Atomic charges of the title compounds computed by Mulliken method and at the B3LYP/6-31G* level of calculation, are illustrated in table 5. The magnitudes of the carbon atomic charges for the compound were found to be both positive and negative.. The magnitude of the hydrogen atomic charges is found to be positive and negative.

Thermodynamic properties

Several thermo dynamical parameters have been calculated by using DFT with6-31G* basis set are given in table 6. Scale factors have been recommended by Minnesota for an accurate prediction determining the zero-point vibrational energies for DFT calculation. The total energy of the molecule is the sum of the translational, rotational, vibrational and electronic energies.

Dipole moment

Dipole moment reflects the molecular charge distribution and is given as a vector in three dimensions. Therefore, it can be used as descriptor to depict the charge movement across the molecule. Direction of the dipole moment vector in a molecule depends on the centers of positive and negative charges. Dipole moments are strictly determined for neutral molecules. Dipole moment values of the title compounds are shown in table 6.

Polarizability and Hyperpolarizability

The polarizabilities and hyperpolarizability characterize the response of a system in an applied electric field. The potential application of the title molecule in the field of nonlinear optics demands the investigation of its structural and bonding features contributing to the hyperpolarizability enhancement, by analyzing the vibrational modes using IR and Raman spectroscopy. Many organic molecules, containing conjugated π electrons are characterized by large values of molecular first hyperpolarizability, were analyzed by means of vibrational spectroscopy (Karpagam *et al.,* 2010; Vijaykumar *et al.,* 2008). The first hyperpolarizability β of this novel molecular system of SCSA are calculated using the ab

initio quantum mechanical method, based on the finite-field approach. In the presence of an applied electric field, the energy of a system is a function of the electric field. First hyperpolarizability (β) is a third rank tensor that can be described by a 3 x 3 x 3 matrix. The 27 components of the 3D matrix can be reduced to 10 components due to the Kleinman symmetry (Kleinman, 1962). The first hyperpolarizability β, dipole moment μ and polarizability α is calculated using 6-31G* basis set on the basis of the finite-field approach. The complete equations for calculating the magnitude of total static dipole moment μ, the mean polarizability αtot, the anisotropy of the polarizability Δα, and the mean first polarizability βo, using the x, y, z components from Gaussian03W output is as follows.

$$\mu_{tot} = \left(\mu_x^2 + \mu_y^2 + \mu_y^2\right)^{1/2}$$

$$\alpha_{tot} = 1/3\left[(\alpha_{xx} + \alpha_{yy} + \alpha_{zz})\right]$$

$$\Delta\alpha = 1/\sqrt{2}\left[(\alpha_{xx} - \alpha_{yy})^2 + (\alpha_{yy} - \alpha_{zz})^2 + (\alpha_{zz} - \alpha_{xx})^2 + 6\alpha_{xz}^2 + 6\alpha_{yz}^2 + 6\alpha_{xy}^2\right]^{1/2}$$

$$\beta_0 - \left[(\beta_{xxx} + \beta_{xyy} + \beta_{xzz})^2 + (\beta_{yyy} + \beta_{yzz} + \beta_{yxx})^2 + (\beta_{zzz} + \beta_{zxx} + \beta_{zyy})^2\right]^{1/2}$$

The polarizability and hyperpolarizability are reported in atomic units (a.u), the calculated values have been converted into electrostatic units (e.s.u) (for α:1 a.u.= 0.1482x 10^{-24} esu, for β:1 a.u. = 8.6393 x 10^{-33} esu). Theoretically calculated values of first hyperpolarizability and dipole moment are as shown in table 7. The large value of hyperpolarizability, β which is a function of the non-linear optical activity of the molecular system, is associated with the intramolecular charge transfer, resulting from the electron cloud movement through π conjugated frame work from electron donor to electron acceptor groups. The physical properties of these conjugated molecules are governed by the high degree of electronic charge delocalization along the charge transfer axis and by the low band gaps. So we conclude that the title molecule is an attractive object for future studies of nonlinear optical properties.

Frontier molecular orbitals (FMOs)

The highest occupied molecular orbitals (HOMO) and the lowest-lying unoccupied molecular orbitals (LUMO) are named as frontier molecular orbitals (FMO). The FMO play an important role in the optical and electric properties, as well as in quantum chemistry (Fleming, 1976). The HOMO – LUMO energy gap of SCSA have been calculated at the B3LYP/6-31G* level and are shown in table 8, which reveals that the energy gap reflect the chemical activity of the molecules. LUMO is an electron accepter, that represents the ability to obtain an electron and HOMO represents the ability to donate an electron. This electronic absorption corresponds to the transition from the ground to the first excited state and is mainly described by 1 electron excitation from the highest occupied molecular orbital to the lowest unoccupied molecular orbital. While the energy of the HOMO is directly related to the ionization potential, LUMO energy is directly related to the electron affinity. The frontier orbitals (HOMO, LUMO) of SCSA, with its energy are plotted in figure 4.

For SCSA,
HOMO energy = -0.220 a.u
LUMO energy = - 0.064 a.u
HOMO – LUMO energy gap = 0.156 a.u

^{13}C and ^{1}H NMR spectral analysis

The isotropic chemical shifts are frequently used as an aid in identification of reactive organic as well as ionic species. Then, gauge –including atomic orbital (GIAO) ^{13}CNMR

and ^{1}HNMR chemical shifts calculations of the title compounds have been carried out by using B3LYP/ functional with 6-31G* basis set. Application of the GIAO (Ditchfield, 1972) approach to molecular systems was significantly improved by an efficient application of the method to the ab initio SCF calculation, using techniques borrowed from analytic derivative methodologies. Relative chemical shifts were estimated by using the corresponding TMS shielding calculated in advanced at the same theoretical level as the reference.

Table.1 Optimized geometrical parameters of SCSA obtained by B3LYP 6/31G* density functional calculations

	Value (A^0)		Value (^{0})
Bond length	**SCSA**	Bond angle	**SCSA**
C1-C2	1.382	C1-C2-C3	121.820
C2-C3	1.412	C2-C3-C4	118.938
C3-C4	1.420	C3-C4-C5	118.468
C4-C5	1.408	C4-C5-C6	121.251
C5-C6	1.384	C2-C1-H7	120.442
C1-H7	1.084	C1-C2-H8	120.999
C2-H8	1.084	C4-C5-H9	117.225
C5-H9	1.084	C5-C6-H10	119.347
C6-H10	1.086	C3-C4-O11	126.370
C4-O11	1.341	C4-O11-H12	113.476
O11-H12	0.977	C2-C3-C13	115.117
C3-C13	1.474	C3-C13-O14	125.904
C13-O14	1.209	C3-C13-O15	111.875
C13-O15	1.392	C13-O15-C16	121.303
O15-C16	1.381	O15-C16-C17	118.312
C16-C17	1.410	O15-C16-C18	121.089
C16-C18	1.395	C16-C17-C19	118.479
C17-C19	1.406	C16-C18-C20	119.765
C18-C20	1.392	C16-C18-H21	119.455
C18-H21	1.081	C17-C19-C22	121.098
C19-C22	1.388	C17-C19-H23	118.510
C19-H23	1.082	C18-C20-H24	119.186
C20-H24	1.085	C19-C22-H25	120.038
C22-H25	1.084	C16-C17-C26	121.785
C17-C26	1.483	C17-C26-O27	126.877
C26-O27	1.219	C17-C26-O28	112.601
C26-O28	1.353	C26-O28-H29	105.640
O28-H29	0.971		

The atom indicated in the parenthesis belongs to SCSA; for numbering of atoms refer figure 1.

Table.2 Definition of internal co-ordinates of SCSA

No	Symbol	Type	Definition
Stretching			
1-12	P_i	C-C	C1-C2,C2-C3, C3-C4, C4-C5,C5-C6, C6-C1, C16-C17,C17-C19, C19-C22,C22-20, C20-C18, C18-C16. C3-C13,C17-C26.
13-14	pi	C-C(a)	
15-22	Qi	C-H	C1-H7, C2-H8, C5-H9, C6-H10, C18-H21, C19-H23, C20-H24, C22-H25.
23-28	qi	C-O	C4-O11, C13-O14, C13-O15,C16-O15,C26-O27, C26-O28.
29-30	Ri	O-H	O11- H12,O28-H29.
Bending			
In- plane bending			
31-34	β_i	C-C-C	C2-C3-C13, C4-C3-C13, C16-C17-C26, C19-C17-C26.
35-50	β_i	C-C-H	C2-C1- H7,C6-C1-H7, C3-C2- H8, C1-C2- H8, C4-C5- H9, C6-C5- H9, C1-C6- H10, C5- C6-H10, C16-C18-H21, C20-C18-H21,C17-C19-H23,C22-C19-H23,C22-C20-H24,C18-C20-H24,C20-C22-H25,C19-C22-H25.
51-54	α_i	C-C-O	C3-C13- O14, C3-C13-O15,C17-C26-O27,C17-C26-O28.
55-56	ρ_i	C-O-H	C4-O11-H12,C26-O28-H29.
57-60	θ_i	C-O	C3-C4-O11,C5-C4-O11,C17-C16-O15,C18-C16-O15.
61	θ_i	C-O-C	C13-O15-C16

62-67	Φ_i	C–C–C (ring1)	C1–C2–C3, C2–C3–C4, C3–C4–C5, C4–C5–C6, C5–C6-C1, C6–C1–C2.
68-73	Φ_i	C–C–C (ring2)	C16-C17– C19, C17–C19–C22, C19–C22– C20, C22–C20–C18, C20–C18–C16,C18-C16-C17.
Out–of–plane bending			
74-75	ω_i	C-C	C13-C3-C2-C4, C26C17-C16-C19.
76-83	ω_i	C-H	H7-C1-C2-C6,H8-C2-C1-C3,H9-C5-C4-C6,H10-C6-C5-C1,H21-C18-C16-C20,H23-C19-C22-C17,H24-C20-C18-C22,H25-C22-C20-C19.
84-85	ω_i	C-O	O11-C4-C5-C3,O15-C16-C17-C18.
Torsion			
86-87	τ_i	C-O-H	C3-C4-O11-H12,C17-C26-O28-H29.
88-91	τ_i	C-O	C2-C3-C13-O14,C4-C3-C13-O15,C16-C17-C26-O27,C19-C17-C26-O28.
92	τ_i	C-O-C	C16-O15-C13-C3.
93	τ_i	O-C-O	O14-C13-O15-C16.
94-99	τ_i	Tring 1	C1–C2–C3-C4, C2–C3–C4-C5, C3–C4–C5-C6, C4–C5–C6-C1, C5–C6-C1-C2, C6–C1–C2-C3.
100-105	τ_i	Tring 2	C16-C17– C19-C22, C17–C19– C22-C20, C19–C22–C20-C18, C22–C20–C18-C16, C20–C18-C16-C17, C18–C16– C17-C19.

For numbering of atoms refer figure 1.

Table.3 Definition of local symmetry coordinates of SCSA

No.	Symbol [a]	Definition [b]
1-12	CC	P_1, P_2, P_3, P_4, P_5, P_6, P_7, P_8, P_9, P_{10}, P_{11}, P_{12}.
13-14	CC(a)	p_{13}, p_{14}.
15-22	CH	Q_{15}, Q_{16}, Q_{17}, Q_{18}, Q_{19}, Q_{20}, Q_{21}, Q_{22},
23-28	CO	q_{23}, q_{24}, q_{25}, q_{26}, q_{27}, q_{28}.
29-30	OH	R_{29},R_{30}.
31-32	bCC	$(\beta_{31}-\beta_{32})/\sqrt{2}$, $(\beta_{33}-\beta_{34})/\sqrt{2}$
33-40	bCH	$(\beta_{35}-\beta_{36})/\sqrt{2}$,$(\beta_{37}-\beta_{38})/\sqrt{2}$, $(\beta_{39}-\beta_{40})/\sqrt{2}$,$(\beta_{41}-\beta_{42})/\sqrt{2}$, $(\beta_{43}-\beta_{44})/\sqrt{2}$,$(\beta_{45}-\beta_{46})/\sqrt{2}$, $(\beta_{47}-\beta_{48})/\sqrt{2}$,$(\beta_{49}-\beta_{50})/\sqrt{2}$.
41-44	bCCO	α_{51}, α_{52}, α_{53}, α_{54}.
45-46	bCOH	ρ_{55}, ρ_{56}.
47-48	bCO	$(\theta_{57}-\theta_{58})/\sqrt{2}$, $(\theta_{59}-\theta_{60})/\sqrt{2}$
49	bCOC	Θ_{61}
50	bring1	$(\Phi_{62}-\Phi_{63}+\Phi_{64}-\Phi_{65}+\Phi_{66}-\Phi_{67})/\sqrt{6}$
51	bring1	$(-\Phi_{62}-\Phi_{63}+2\Phi_{64}-\Phi_{65}-\Phi_{66}+\Phi_{67})/\sqrt{12}$
52	bring1	$(\Phi_{62}-\Phi_{63}+\Phi_{64}-\Phi_{65})/2$
53	bring2	$(\Phi_{68}-\Phi_{69}+\Phi_{70}-\Phi_{71}+\Phi_{72}-\Phi_{73})/\sqrt{6}$
54	bring2	$(-\Phi_{68}-\Phi_{69}+2\Phi_{70}-\Phi_{71}-\Phi_{72}+2\Phi_{73})/\sqrt{12}$
55	bring2	$(\Phi_{68}-\Phi_{69}+\Phi_{70}-\Phi_{71})/2$
56-57	ωCC	ω_{74}, ω_{75}.
58-65	ωCH	ω_{76}, ω_{77}, ω_{78}, ω_{79}, ω_{80}, ω_{81} ω_{82}, ω_{83}.
66-67	ωCO	ω_{84}, ω_{85}.
68-69	tCOH	τ_{86},τ_{87}.
70-73	tCO	τ_{88},τ_{89},τ_{90},τ_{91}.
74	tCOC	τ_{92}.
75	tOCO	τ_{93}.
76	tring1	$(\tau_{94}+\tau_{95}+\tau_{96}+\tau_{97}+\tau_{98}+\tau_{99})/\sqrt{6}$
77	tring1	$(\tau_{94}+\tau_{95}+\tau_{96}+\tau_{97})/2$
78	tring1	$(-\tau_{94}+2\tau_{95}-\tau_{96}-\tau_{97}+2\tau_{98}-\tau_{99})/\sqrt{12}$
79	tring2	$(\tau_{100}+\tau_{101}+\tau_{102}+\tau_{103}+\tau_{104}+\tau_{105})/\sqrt{6}$
80	tring2	$(\tau_{100}+\tau_{101}+\tau_{102}+\tau_{103})/2$
81	tring2	$(-\tau_{100}+2\tau_{101}-\tau_{102}-\tau_{103}+2\tau_{104}-\tau_{105})/\sqrt{12}$

[a]These symbols are used for description of the normal modes by PED in table 4.
[b]The internal coordinates used here are defined in table 2.

Table.4 Observed and B3LYP/6−31G*level Calculated vibrational frequency (cm^{-1}) of SCSA

Sl. No	Symmetry species	Observed frequencies (cm^{-1})		Calculated frequencies (cm^{-1}) with B3LYP/6−31G* force field				TED (%)among type of internal coordinates
		Infrared	*Raman*	Un scaled	Scaled	IR[a] (A_i)	Raman[b] (I_i)	
1	A	3470	-	3628	3471	91.545	143.735	OH (98)
2	A	3235	-	3418	3271	790.451	223.980	OH (99)
3	A	-	3088	3255	3115	0.324	76.201	CH (99)
4	A	3087	-	3237	3097	2.715	120.358	CH (98)
5	A	3072	-	3223	3084	10.465	173.958	CH (99)
6	A	-	3072	3216	3077	7.444	109.896	CH (100)
7	A	-	3054	3211	3072	15.448	194.762	CH (100)
8	A	3026	-	3205	3067	10.995	130.301	CH (100)
9	A	2893	-	3195	3057	3.467	77.737	CH (100)
10	A	2870	-	3186	3049	8.413	92.109	CH (100)
11	A	-	1742	1811	1733	445.824	79.471	CC(73),bCH(11)
12	A	1739	-	1796	1718	265.883	106.302	CO(68),bCC(26)
13	A	-	1612	1672	1600	126.542	73.327	CC(60),CCa(17), bCOC(15)
14	A	1609	-	1655	1583	45.513	54.973	CC(72), bring(12)
15	A	-	1585	1632	1561	41.839	18.119	CO(55),bCH(15), CC(10)
16	A	1580	-	1618	1548	35.605	37.480	CO(16),CC(14), bCO(10)
17	A	-	1466	1532	1466	81.030	7.107	CO(68), bCC(26)
18	A	1460	-	1527	1461	128.430	9.498	CC(68), bCOC(11),bring(11)
19	A	1450	-	1507	1442	35.474	10.787	CC(48), bCCO(14),bCH(11)
20	A	1413	-	1487	1423	38.143	3.884	CC(31),bring(17), bCH (14)
21	A	1333	-	1398	1337	126.047	10.453	CC(52), bCO(20), bring (14)
22	A	-	1322	1389	1329	27.127	41.904	CC(58), bCC(13),bCH(11)
23	A	1301	-	1369	1310	3.114	3.523	CC(65), bCOC(21)
24	A	-	1279	1355	1296	6.867	8.358	CO(55), bring(10)
25	A	-	1249	1307	1250	10.783	1.600	CC(56), bCCO(11),bCOH(11)

26	A	1247	-	1301	1245	292.523	12.173	bCOH(47), CC(12)
27	A	-	1204	1275	1220	208.224	27.763	CO(68), bCC(26)
28	A	1200	-	1244	1190	309.173	55.933	bCOH(64), bCO(20)
29	A	-	1169	1212	1159	277.125	26.514	CC(68), bCH(11),bCC(11)
30	A	-	1160	1207	1155	79.425	60.050	CC(41),bring(17), bCH (14)
31	A	1158	-	1192	1140	40.215	23.138	bCC(78)
32	A	1129	-	1181	1130	65.569	22.147	bCH(23), bCCO(14), bring(12), CC(11)
33	A	1115	-	1171	1120	37.097	0.872	bCCO(23), bCH(14), CH(15), CC(11)
34	A	1088	-	1129	1080	47.802	5.586	bCCO(23), bCC(14), bring(12), CCa(11)
35	A	1067	-	1096	1048	219.683	5.390	bCC(48),OH(16)
36	A	-	1036	1080	1033	96.643	47.197	CCa(67),bCC(12), bCH(11)
37	A	1026	-	1072	1025	10.090	3.521	CCa(45),bCO(18), bCH(13)
38	A	979	-	1043	998	280.684	8.138	bCH(23), bCO(14), CC(11)
39	A	936	-	998	955	0.154	0.043	bCH(34), bCCO(14), bring(12), CO(11)
40	A	-	930	991	948	0.137	0.086	bCCO(64), bCO(20)
41	A	-	901	976	934	1.023	0.538	bCH(23), bCCO(14), CH(17)
42	A	900	-	971	929	1.924	1.247	bCH(23), bCCO(14), bring(12), CC(11)
43	A	-	862	896	857	3.095	3.331	ωCH (57), tring(18)
44	A	-	823	878	840	1.312	4.804	bCOC(64), bCO(20)
45	A	820	-	876	838	3.330	2.129	ωCC (57), tring(18)
46	A	810	-	850	813	1.630	2.201	bCH(63), bCC(20)
47	A	-	805	836	800	13.611	25.243	bCH(63), bCC(20)
48	A	-	770	800	765	1.007	1.462	bCH(63), bCC(20)
49	A	757	-	790	756	5.141	2.424	bring (72)
50	A	-	752	766	733	52.767	3.687	bCCO(23), bCO(14), bring(12), CC(11)

51	A	751	-	761	728	60.708	12.269	bring (63)
52	A	-	695	757	724	9.542	3.263	ωCO(60), bCC(20
53	A	694	-	712	681	48.613	3.281	tCOH(60), ωCC(20)
54	A	671	-	699	668	20.421	1.395	bring (48), CC(11)
55	A	663	-	674	645	12.430	8.393	bring (48), CC(11)
56	A	-	662	654	625	108.435	0.694	tCO(60), ωCH(20)
57	A	598	-	623	596	35.548	1.320	ωCO(60), bCC(20
58	A	-	594	606	579	65.102	6.901	tring(54), ωCH(33)
59	A	580	-	598	572	3.921	9.634	bring (48), CC(11)
60	A	-	566	570	545	6.074	12.423	ωCH(60), bCC(20)
61	A	-	555	545	521	2.254	1.151	ωCH(62), tring(15)
62	A	549	-	533	510	2.363	2.137	bCH(43), bring(22),bCC(22)
63	A	-	530	530	507	4.221	0.694	ωCH(62), tring(15)
64	A	498	-	526	503	18.604	0.870	ωCC (57), tring(18)
65	A	-	484	442	422	0.084	0.179	tCOH(60), ωCC(20)
66	A	-	447	432	413	5.128	1.558	bring (48), CC(11)
67	A	-	380	416	398	4.199	2.906	tring(54), CH(33)
68	A	-	365	387	370	1.536	3.576	ωCH(62),tring(15)
69	A	-	330	348	333	1.790	1.577	ωCH(62), tring(15)
70	A	-	276	303	289	4.955	0.431	ωCH(62), tring(15)
71	A	-	269	275	263	0.326	3.380	bCO(73), bOH(13)
72	A	-	248	252	241	0.452	3.589	bCO(73), bCC(12)
73	A	-	214	236	225	0.752	0.578	ωCH(62),tCOH(15)
74	A	-	207	209	200	1.881	1.376	tCO(60), ωCH(20)
75	A	-	189	194	185	0.957	3.570	tCO(60), ωCH(20)
76	A	-	163	168	160	2.622	4.034	ωCH(60), bCC(20)
77	A	-	132	146	139	2.691	0.998	tring (70)
78	A	-	120	134	128	0.402	0.355	tring (62),tCOH(15)
79	A	-	117	100	95	0.965	5.883	tCOC(60), ωCH(20)
80	A	-	107	63	60	1.303	4.052	tring (70)
81	A	-	98	62	59	0.923	3.952	tring(54), ωCH(33)

Abbreviations used: R: ring; ss:symmetric stretching; b:bending; ω:ωagging; t:torsion;
Contributions larger than 10% are given.

[a]Relative absorption intensities normalized with highest peak absorption equal to 1.0.

[b]Relative Raman intensities calculated by E.2 and normalized to 100

Table.5 Atomic charges for optimized geometry of SCSA

Atoms[a]	B3LYP/6-31G*
	Mulliken
	SCSA
C1	-0.101794
C2	-0.101428
C3	-0.012593
C4	0.298866
C5	-0.104247
C6	-0.077557
H7	0.090625
H8	0.120984
H9	0.096051
H10	0.090659
O11	-0.572793
H12	0.369479
C13	0.594277
O14	-0.468374
O15	-0.570761
C16	0.317522
C17	0.012437
C18	-0.073220
C19	-0.111712
C20	-0.089654
H21	0.121229
C22	-0.083239
H23	0.126550
H24	0.102853
H25	0.099050
C26	0.573626
O27	-0.489288
O28	-0.490461
H29	0.332915

[a]The atoms indicated in the parenthesis belongs to SCSA; for numbering of atoms refer figure 1.

Table.6 Theoretically computed energies (a.u), zero-point vibrational energies (kcal/mol), rotational constants (GHz), entropies (cal/mol-Kelvin) and dipole moment (Debye)

Parameters	**B3LYP/6-31G***
	SCSA
Total energy	-915.6845
Zero-point energy	135.31962
Rotational constant	0.77367
	0.23903
	0.19152
Entropy	
Total	126.864
Translational	42.544
Rotational	33.473
Vibrational	50.847
Dipole moment	2.4888

Table.7 Nonlinear optical properties of SCSA calculated using B3LYP/6-31G* basis set

NLO behavior	**SCSA**
Dipole moment (μ)	1.5820 Debye
Mean polarizablity (α)	3.516×10^{-24} esu
Anisotropy of the polarizability (Δα)	88.384
First hyper polarizability (β_o)	1.0735×10^{-30} esu

Table.8 HOMO – LUMO energy value calculated by B3LYP/6-31G*

Parameters	**B3LYP/6-31G***
	SCSA
HOMO	-0.220
LUMO	-0.064
HOMO -LUMO	0.156

Table.9 Theoretical and experimental 1H NMR and 13C NMR spectra of SCSA (with respect to TMS, all values in ppm) for B3LYP/6-31G*

Atoms	SCSA	
	Exp	**Cal**
C1	119.53	121.049
C2	130.73	138.445
C3	111.93	117.838
C4	161.96	163.505
C5	117.69	123.152
C6	136.42	138.544
C13	168.96	166.136
C16	150.45	157.304
C17	124.07	123.262
C18	122.48	129.067
C19	132.74	136.338
C20	134.91	137.232
C22	126.61	127.125
C26	169.76	167.537
H7	6.91	7.723
H8	8.12	9.070
H9	7.01	7.834
H10	7.50	8.306
H12	10.25	10.942
H21	7.25	8.728
H23	8.05	9.212
H24	7.63	8.516
H25	7.37	8.158
H29	10.73	6.700

For numbering of atoms refer figure 1.

Fig.1 Molecular model of SCSA along with numbering of atoms

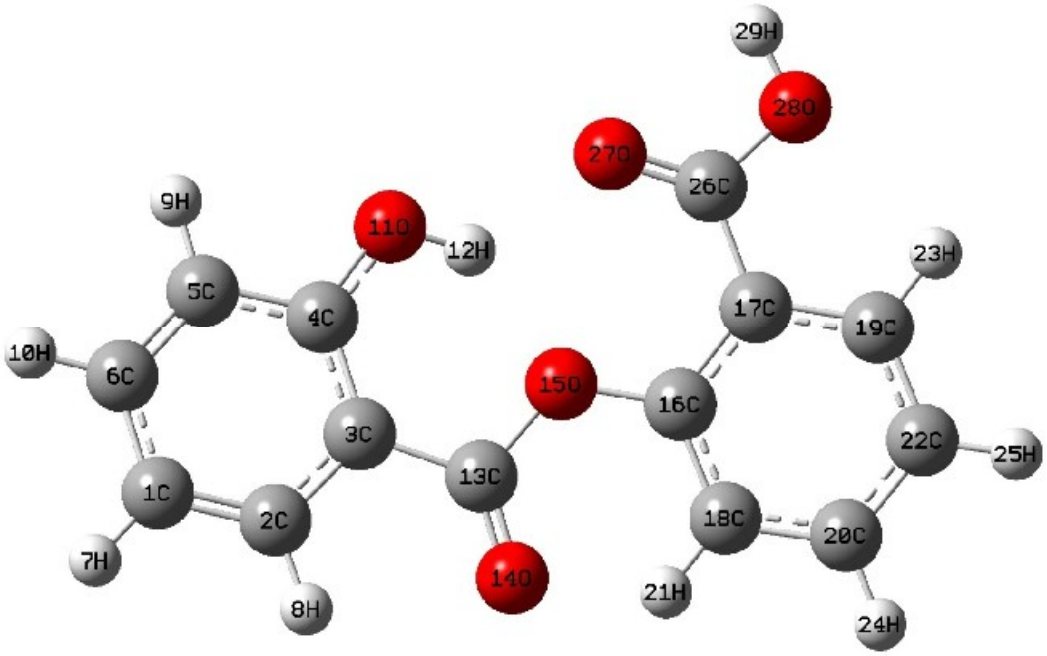

Fig.2 FTIR spectra of SCSA (a) calculated (b) observed with B3LYP/6-31G*

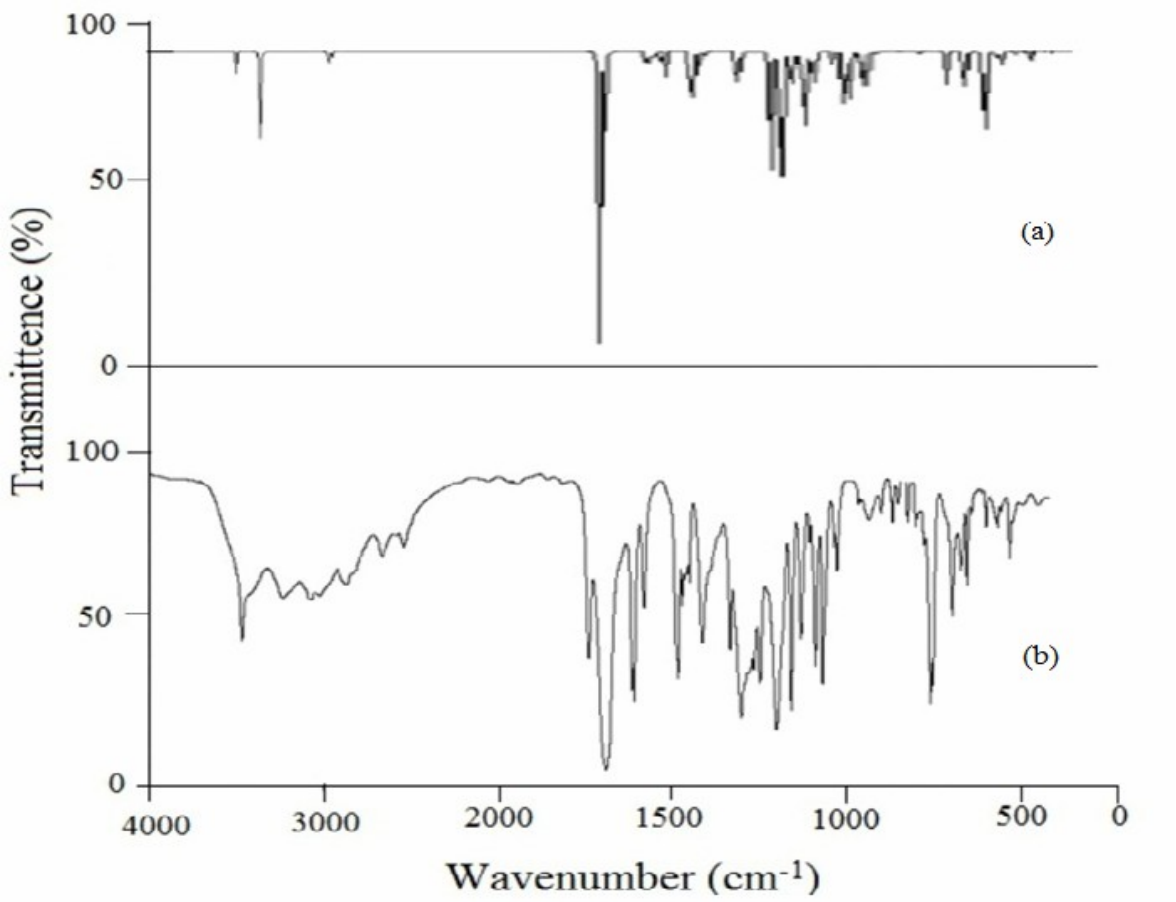

(a) Calculated with B3 LYP/6-31G*
(b) Observed with KBr disc

Fig.3 FT-Raman spectra of SCSA (a) calculated (b) observed with B3LYP/6-31G*

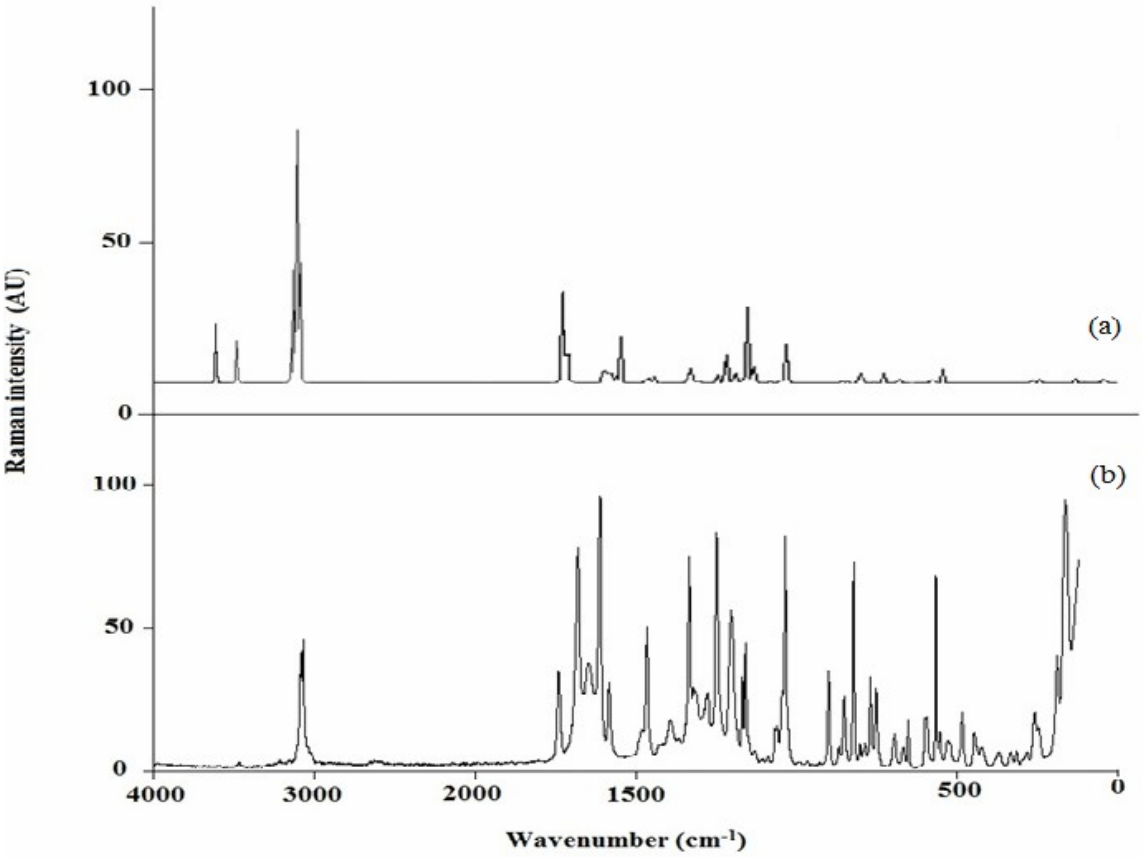

(a) Calculated with B3 LYP/6-31G*
(b) Observed with KBr disc

Fig.4 HOMO and LUMO plot of SCSA

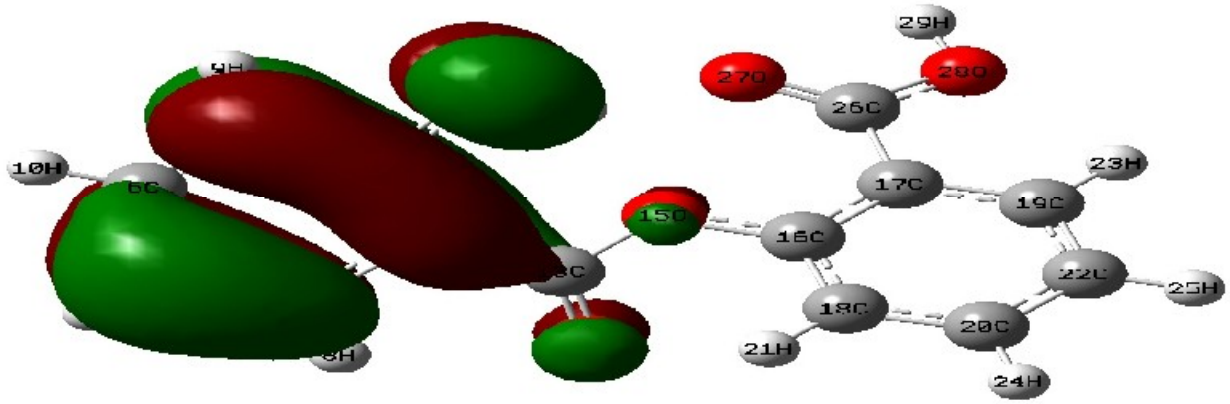

(a) E_{HOMO} = - 0.220 a.u

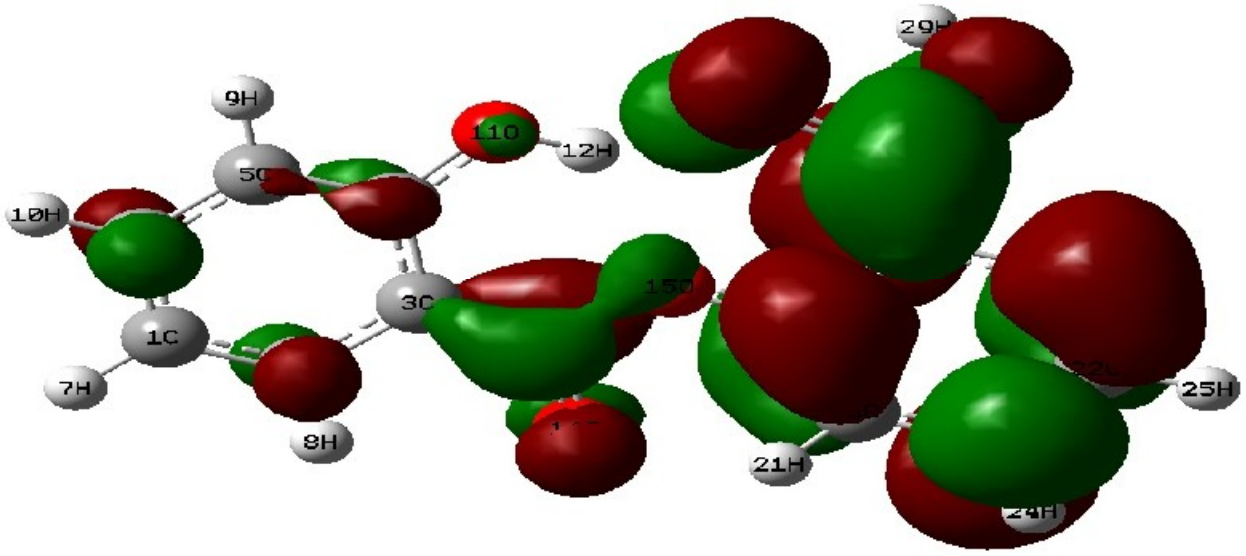

(b) E_{LUMO}= - 0.064 a.u
$\Delta E_{HOMO-LUMO}$= 0.156 a.u

Fig.5 The Linear regression between experimental and theoretical 13 C (a) 1H (b) NMR Chemical Shift for SCSA

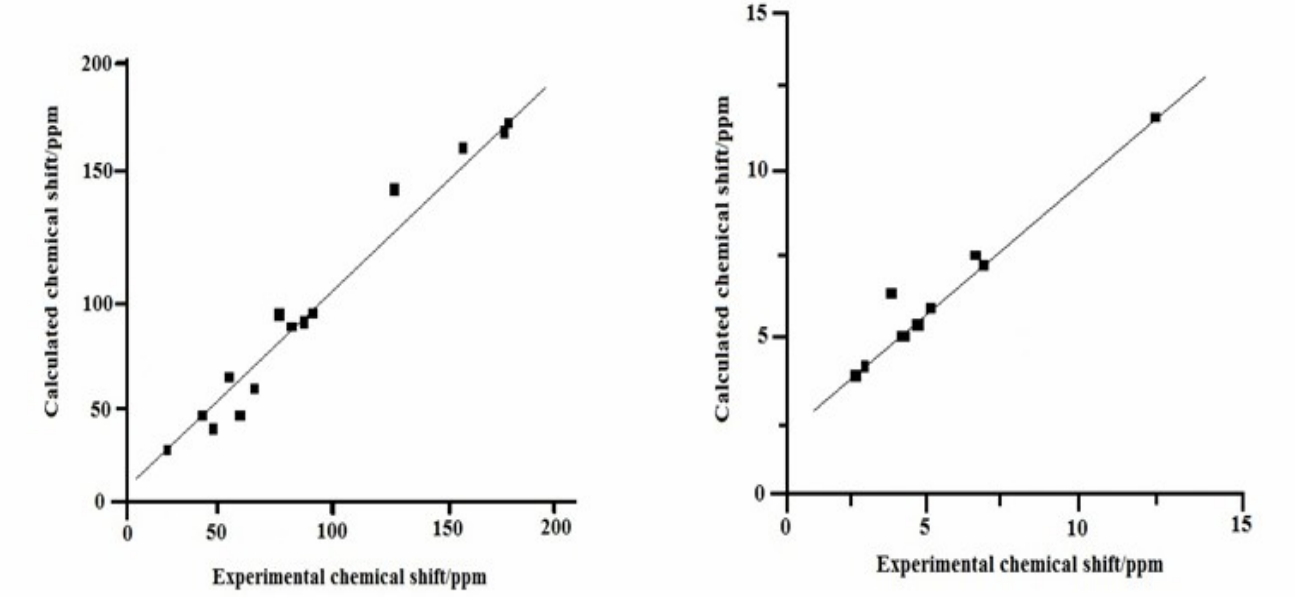

Experimental and theoretical chemical shifts of SCSA in ^{13}CNMR and ^{1}HNMR spectra were recorded and the obtained data are presented in table 9. The linear correlations between calculated and experimental data of ^{13}CNMR and ^{1}HNMR spectra are noted. Correlation coefficients of ^{13}CNMR and ^{1}HNMR are 1.0629 and 0.9457 for SCSA. The data shows a good correlation between predicted and observed proton and carbon

chemical shifts. The correlations of NMR spectra are presented in figure 5 for SCSA. The range of the ^{13}CNMR chemical shifts for a typical organic molecule usually is>100 ppm (Kalinowski *et al.,* 1988; Pihlaja and Kleinpeter, 1994) and the accuracy ensures reliable interpretation of spectroscopic parameters. In the present study, the ^{13}CNMR chemical shifts in the ring for SCSA are>100 ppm, as they would be expected.

Conclusion

In the present work, the optimized molecular structure of the stable conformer, thermodynamic properties and vibrational frequencies of the title compound have been calculated by DFT method using B3LYP/6-31G* basis set. The theoretical results were compared with the experimental vibrations. The calculated HOMO and LUMO energies show that charge transfer occurs within the molecule. ^{1}H and ^{13}C NMR chemical shifts have been compared with experimental values. As a result, all the vibrational frequencies were calculated and scaled values (with 6-31G* basis set) have been compared with experimental FTIR and FT-Raman spectra. The observed and the calculated frequencies are in good agreement. Furthermore, the nonlinear optical, first-order hyperpolarizabilities and total dipole moment properties of the molecules show that the title molecules are an attractive object for future studies of nonlinear optical properties.

References

Becke, A.D. 1988. Density-functional exchange-energy approximation with correct asymptotic behavior. *Phys. Rev. A*, 38: 3098–3100.

Bellamy, L.J. 1975. The infrared spectra of complex molecules, 3rd edn. Wiley, New York.

Blom, C.E., Altona, C. 1976. Application of self-consistent-field ab initio calculations to organic molecules. *Mol. Phys.*, 31: 1377.

Bowman, W.D., Spiro, T.G., Bhem. J. 1980. *J. Chem. Phys.*, 73: 5482.

Cheeseman, J. R., Trucks, G. W., Keith, T. A., Frisch, M. J. 1996. A comparison of models for calculating nuclear magnetic resonance shielding tensors. *J. Chem. Phys.*, 104: 5497.

Ditchfield, R. 1972. Molecular orbital theory of magnetic shielding and magnetic susceptibility. *J. Chem. Phys.*, 56: 5688.

Fleming, I. 1976. Frontier orbitals and organic chemical reactions. Wiley, London.

Frisch, A.., Nielsen, A.B., Holder, A.J., Gauss view users manual, Gaussian Inc., Pittsburgh.

Frisch, M.J., Trucks, G.W., Schlegel, H.B., Scuseria, G.E., Robb, M.A., Cheeseman, J.R., Montgomery, J.A., Jr., Vreven, T., Kudin, K.N., Burant, J.C., Millam, J.M., Iyengar, S.S., Tomasi, J., Barone, V., Mennucci, B., Cossi, M., Scalmani, G., Rega, N., Petersson, G.A., Nakatsuji, H., Hada, M., Ehara, M., Toyota, K., Fukuda, R., Hasegawa, J., Ishida, M., Nakajima, T., Honda, Y., Kitao, O., Nakai, H., Klene, M., Li, X., Knox, J.E., Hratchian, H.P., Cross, J.B., Bakken, V., Adamo, C., Jaramillo, J., Gomperts, R., Stratmann, R.E., Yazyev, O., Austin, A.J., Cammi, R., Pomelli, C., Ochterski, J.W., Ayala, P.Y., Morokuma, K., Voth, G.A., Salvador, P., Dannenberg, J.J., Zakrzewski, V.G., Dapprich, S., Daniels, A.D., Strain, M.C., Farkas, O., Malick, D.K., Rabuck, A.D., Raghavachari, K., Foresman, J.B.,

Ortiz, J.V., Cui, Q., Baboul, A.G., Clifford, S., Cioslowski, J., Stefanov, B.B., Liu, G., Liashenko, A., Piskorz, P., Komaromi, I., Martin, R.L., Fox, D.J., Keith, T., Al-Laham, M.A., Peng, C.Y., Nanayakkara, A., Challacombe, M., Gill, P.M.W., Johnson, B., Chen, W., Wong, M.W., Gonzalez, C., Pople, J.A., Gaussian 03, Revision E.01, Gaussian, Inc., Wallingford, CT, 2004.

George, S. 2001. Infrared and Raman characteristic group frequencies, tables and charts, 3rd edn., Wiley, Chichester.

Hawley, S. A., Fullerton, M. D., Ross, F.A., Schertzer, J.D., Chevtzoff, C., Walker, K.J., Peggie, M.W., Zibrova, D. *et al.* 2012. *Science,* 336(6083): 918–22.

Hehre, W.J., Random, L., Schleyer, P.V.R., Pople, J.A. 1986. Ab initio Molecular Orbital Theory, Wiley, New York.

Hess, B.A., Schaad, J., Carsky, P., Zahraduik, R. 1986. *Chem. Rev.,* 86: 709.

Kalinowski, H.O., Berger, S., Barun, S. 1988. C-13 NMR spectroscopy. Chichester, John Wiley and Sons.

Karpagam, J., Sundaraganessan, N., Sebastian, S., Manoharan, S., Kurt, M., Raman, J. 2010. *Spectros.*, 41: 53–62.

Keresztury, G., Holly, S., Varga, J., Besenyei, G., Wang, A.Y., Durig, J.R. 1993. *Spectrochim. Acta A,* 49: 2007–2026.

Kleinman, D.B. 1962. *Phys. Rev.*, 126: 1977–1979.

Lee, C., Yang, W., Parr, R.G. 1988. *Phys. Rev. B*, 37: 785–789.

Pihlaja, K., Kleinpeter, E. (Eds), Carbon-13 chemical shifts in structural and stereo chemical analysis, VCH Publishers, Deerfield Beach, FL.

Polavarapu, P.L. 1990. *J. Phys. Chem.*, 94: 8106–8112.

Pulay, P., Fogarasi, G., Pongor, G., Boggs, J.E., Vargha, A. 1983. *J. Am. Chem. Soc.*, 105: 7037–7047.

Pulay, P., Zhou, X., Fogarasi, G., Fransto, R. (Eds). 1993. NATO AS Series, Vol. C, 406, Kluwer, Dordrecht. Pp. 99.

Rauhut, G., Pulay, P. 1995. *J. Phys. Chem.*, 99: 3093–3100.

Sathyanarayan, D.N., Vibrational spectroscopy—theory and applications, 2nd edn. New Age International (P) Limited Publishers, New Delhi.

Shin, D.N., Hahn, J.W., Jung, K.H., Ha, T.K., Raman, J. 1998. *Spectrosc,* 29: 245.

Silverstein, M., Clayton Bassler, G., Morril, C. 1981. Spectroscopic identification of organic compounds. John Wiley, New York.

Socrates, G. 2001. Infrared and Raman characteristic group frequencies—Tables and Charts, 3rd edn. Wiley, New York.

Sundius, T. 1990. *J. Mol. Struct.*, 218: 321–326.

Sundius, T. 2002. *Vib. Spectrosc.*, 29: 89–95.

Varsanyi, G. 1969. Vibrational spectra of benzene derivative. Academic Press, New York.

Varsanyi, G. 1974. Assignments of vibrational spectra of seven hundred benzene derivatives, Vols. 1–2, Adam Hilger.

Vijayakumar, T., Joe, H., Nair, C.P.R., Jayakumar, V.S. 2008. *Chem. Phys.*, 343: 83.

Wang, Y., Saebar, S., Pittman, C.U. 1993. *J. Mol. Struct. Theochem.*, 281: 91–98.

Wilson,E.B., Decius, J.C., Cross, P.C. 1980. Molecular vibrations, Dover Publ. Inc., NewYork.

Wolinski, K., Hinton, J.F., Pulay, P. 1990. *J. Phys. Chem. Soc.*, 112: 8251.

Ziegler, T. 1991. *Chem. Rev.*, 91: 651.